RSC Advances



This is an *Accepted Manuscript*, which has been through the Royal Society of Chemistry peer review process and has been accepted for publication.

Accepted Manuscripts are published online shortly after acceptance, before technical editing, formatting and proof reading. Using this free service, authors can make their results available to the community, in citable form, before we publish the edited article. This Accepted Manuscript will be replaced by the edited, formatted and paginated article as soon as this is available.

You can find more information about *Accepted Manuscripts* in the **Information for Authors**.

Please note that technical editing may introduce minor changes to the text and/or graphics, which may alter content. The journal's standard <u>Terms & Conditions</u> and the <u>Ethical guidelines</u> still apply. In no event shall the Royal Society of Chemistry be held responsible for any errors or omissions in this *Accepted Manuscript* or any consequences arising from the use of any information it contains.



Insights on the Combustion and Pyrolysis behavior of Three Different Rank Coals using Reactive Molecular Dynamic Simulation

Sanjukta Bhoi, Tamal Banerjee*, Kaustubha Mohanty*

Department of Chemical Engineering, Indian Institute of Technology Guwahati, Guwahati – 781039, India.

*Corresponding author. Email: kmohanty@iitg.ernet.in (K. Mohanty); tamalb@iitg.ernet.in (T. Banerjee)

Tel.: 91-361-2582267/66; Fax: 91-361-2582291

Abstract

The process of combustion and pyrolysis of coal can be considered to be convoluted where numerous intermediates are expected to form during the course of reaction. In this work, we have investigated the reactive products using the ReaxFF force field for three different rank (low to high) coals namely lignite, bituminous, and anthracite. It was observed that during the pyrolysis and combustion processes, the gases CO and CO₂ were predominant. The formation rate of CO and CO₂ was found to be higher for lignite coal which agreed with the experimental trend reported in literature. In a similar manner, the fraction of CO and CO₂ was found to be higher in pyrolysis process. Further a large number of principal intermediates such as methane, ethane and ethylene are also generated for low to high rank (lignite, bituminous, and anthracite) of coal. The pyrolysis and combustion processes were affected by temperature (2000 K-4000 K) with respect to the formation of various intermediates (methane, ethane and ethylene). They were found to be throughout high irrespective of the rank of coal. A higher temperature (2000 K-4000 K) was adopted in the reactive molecular dynamics (MD) simulation so as to visualize the chemical reactions within a computational affordable time.

Key word: Coal, Combustion, Pyrolysis, Reactive force field

1. Introduction

Coal is a naturally occurring carbonaceous material which is one of the most important sources for energy production. Approximately 40% of worldwide electricity is produced from coal. It generally ranges from brown to black sedimentary rock composed mainly of organic or inorganic compounds.^{1,2} It has a complex structure and contains functional groups such as free hydroxyl, phenolic, carboxyl, carbonyl and ether. On combustion and pyrolysis, it evolves gases such as CO, CO₂, SO₂ and N₂. Further coal produces a wide range of other pollutants (solid as well as gases) with the functional groups as mentioned above. These studies are difficult to perform in the lab scale.^{3,4} The reaction mechanism explains the details of the consumption of oxygen; and formation of the gas and solid phase oxidation products. The solid oxidation products are usually the phenolic compounds which are separated from coal tar.⁵⁻¹¹

Coal with a higher oxygen content is expected to be more reactive towards gaseous oxygen and can produce large amount of CO₂ and CO upon heating.¹² The heating rate of coal depends on the coal rank where the heating value is low for low rank coal. Further the gaseous yield of CH₄, C₂H₄, and C₂H₆ is also high for low-rank coal as compared to high-rank coal.¹³⁻¹⁶ Irrespective of temperature; the ratio for the formation rate of CO to CO₂ rapidly decreases for high-rank coals. The low-rank coal oxidizes at a high temperature, where the formation behaviour of CO and CO₂ were found to vary with temperature.¹⁰⁻¹⁷ The hydrogen production rate is high for low-rank coal which gives a lower calorific value due to the loss of volatile components.^{18,19}

Therefore to understand the combustion phenomena, the chemical kinetics and thermodynamic models are important aspects .²⁰ Hence it is very essential to study the combustion phenomena even though the detailed structural model of coal or char is

complicated and complex.²¹ Recently a complex structure of coal and char was described by experimental and atomistic simulation.²² This work has opened pathways in understanding the combustion and pyrolysis phenomena of coal which otherwise was impossible few years ago. Simulation methods based on reactive force field thereby becomes a viable tool for studying combustion processes. In our earlier work, we have already described the ReaxFF simulation involving the fundamental reaction mechanism of a representative structure of brown coal.²³ The ReaxFF simulation are accurately close to quantum mechanics (QM) as well as experimental results.^{23,24} A common advantage for both MD and ReaxFF is that the force field parameters are easily obtained from QC (Quantum Chemical) calculations which are computationally affordable.

One of the major problems encountered by coke oven batteries has been the continuous deterioration in quality of coal resulting in coke with high ash content and poor strength. This has contributed to phenomenal increase in the demand of coke in blast furnaces in developing countries. Coke having both ash and sulphur content are linearly dependent on the coal used for its production. Thus, an important objective for studying coal combustion and pyrolysis is to evaluate the fixed carbon in the fuel portion of coke or coal. Higher the fixed carbon, the higher the thermal value of coke and lower the environment impact. While combustion of coal is primarily used for power generation, its use is also manifested in other domains such as material construction, town gas, and iron and steel industry. Similarly, coal pyrolysis contributes multiple products such as gas, liquid, and char. The gas, liquid, and char produced from the coal can further be used as fuel oil, chemical feedstock, boiler feedstock and as a raw material for iron. It also plays a vital role in the production of liquid fuels and chemicals. However, an increase in coal utilization results in greenhouse gas emissions from fossil fuel-fired power generation. The greenhouse gas emissions primarily carbon dioxide

and carbon monoxide thus needs to be quantified first and then reduced by improving efficiency in gasification process.^{2,4-6}

In this context, Reactive MD such as ReaxFF²⁵ has been developed with force fields²⁶⁻³⁴ for large scale systems to describe the bond order, bond distance and bond dissociation energy for the total atomic structure. The kinetics and initial reaction mechanism for hydrocarbons such as coal and algae was earlier studied with the help of ReaxFF within a computational affordable time.^{24,26-34} Recently using Illinois No. 6 coal, ReaxFF described the pyrolysis simulations for a large-scale (>50,000 atoms) molecular model based on experimental data. This was performed to investigate the effect of sulfur content on the pyrolysed coal structure.³⁵⁻³⁷ Similarly, Wang et al.³² described pyrolysis and combustion process of n-dodecane, while Liu et al.³⁸ described the initiation mechanism; kinetics of pyrolysis; and combustion of 1,6-dicyclopropane-2,4-hexyne. Further the macro-model for the thermal decomposition of Morwell brown coal and lignite were described and validated with experimental studies.^{31,39}

Therefore, looking at the coal combustion and pyrolysis, an attempt has been made to predict the quantitative formation of both: major (CO/CO₂) and minor (CH₄, C₂H₄, C₂H₆) products from reactive force field calculations. It should be noted that some of the available kinetic chemical models are very expensive and time consuming. Keeping the above advantages in mind, ReaxFF was used in this work to predict the reaction mechanism for the coal having varying rank such as lignite, bituminous and anthracite. By using ADF software, all the ReaxFF MD simulations were implemented.⁴⁰ The intermediate products formed or evolved from the reaction were then studied in detail. Thereafter comparison of combustion behaviour for all the three coals was done with available experimental data.

2. Computational Details

2.1 ReaxFF

ReaxFF²⁵ was developed for bond dissociation and formation using molecular dynamic simulation. The force field parameters are derived from the quantum mechanics (QM) and are then directly applied to the system. ReaxFF combines quantum mechanics (QM) and classical mechanics models. It is based on the semi-empirical interaction potential where the potential energy of the system is described by different energies of the system (Eq. (1)). Thus ReaxFF is a bond order dependent force field where the bond orders are calculated from the interatomic distances which are updated at every iteration during reactive MD simulation. The total energy of the system is thus the sum of partial non-bonded and covalent interaction energy. The total energy of the system is described by equation (1),

$$E_{\textit{system}} = E_{\textit{bond}} + E_{\textit{over}} + E_{\textit{under}} + E_{\textit{val}} + E_{\textit{pen}} + E_{\textit{tors}} + E_{\textit{conj}} + E_{\textit{vdWaals}} + E_{\textit{Coulomb}} \tag{1}$$

Where, E_{system} is the potential energy of the system which describes the interaction between the particles of the systems, E_{bond} represents the bond energy due to the interatomic distance between a pair of atoms, E_{over} and E_{under} represents over- and under- coordinated energy. E_{val} is the valence angle energy for valence angle i-j-k, where i, j, k are location for three atoms. E_{tors} represent the torsion energy i.e. the position where bond order tends to zero and greater than one. E_{conj} denotes the conjugate effect of the molecular energy and $E_{vdlWaals}$ the non-bonded van der Waals interaction. Finally $E_{Coulomb}$ represents the Coulombic interaction between all atom pairs respectively. The interaction potential is further divided into non-reactive and reactive potentials. A detailed description of the ReaxFF force field is described in our previous work²³ and reviewed by van Duin et al.;²⁵ hence it is not discussed in the current text.

2.2 Pyrolysis Process

The structures of the three different types of coal are taken from literature⁴¹⁻⁴⁴ and are given in Fig. 1. Eighteen anthracite coal molecules, 45 bituminous coal molecules and 16 lignite coal molecules were randomly placed in a periodic box of 60×60×60 Å, 56×56×56 Å and 44×44×44 Å with densities having 0.08 g/cm³, 0.1 g/cm³ and 0.2 g/cm³ respectively. The varying numbers of coal molecules were taken so as to make the number of atoms equal in each case. This allows a uniform comparison for anthracite, bituminous and lignite coal properties. The C/H/O/N/S/B force field was used to study the ReaxFF reactive simulation.³⁵

Initially, the system was minimized at a lower temperature of 10 K in a NVE ensemble. The energy minimization was conducted using NVE ensemble for 10 ps with a time step of 0.25 fs to optimize the intermolecular interaction and prepare the structure of the coal for longer simulation. The process is a non-reactive process in which simply the overlap of assembly of atoms (if any) are detected and subsequently corrected. After minimization, they are equilibrated in NVT ensemble for 5 ps with a time step of 0.1 fs. The equilibration step is required so as to distribute the extra degree of freedom i.e. kinetic energy to the potential energy contribution. The reactive simulations were then used to simulate the final structure at a temperature range of 2000 K to 4000 K.

Further the C-O and O-H bond parameters were switched off during the equilibration simulations to prevent reaction occurrence. For this the ensemble was taken to the target temperature slowly with an interval of 500 K for 200 ps. This is done so as to avoid the sudden jump of kinetic energy. The heating rate would eventually not affect the reaction mechanism, but only alter the time at which the reactant begins to decompose. Using Berendsen thermostat, temperature was controlled with a damping constant of 100 fs. A 0.25 fs time step along with a total time of 200 ps was used to study the pyrolysis process. The total time (200 ps) and time step (0.1 fs) values were chosen, as the thermal

Page 8 of 37

decomposition occurred at a small time, which is observed in literature³¹⁻³³. This also gives reasonable descriptions for the oxidation reaction of hydrocarbon.²⁹ For the analysis of the intermediates and products formed during the MD simulation, a 0.3 bond order cut-off was used for the identification of the molecular species.

2.3 Combustion Process

For the combustion process, systems were created at densities of 0.08 g/cm³, 0.1 g/cm³ and 0.2 g/cm³ respectively. Here the systems comprises of (a) 14 anthracite coal molecules (b) 35 bituminous coal molecules and (c) 12 lignite coal molecules, placed in periodic boxes of dimension 93×93×93 Å, 79×79×79 Å, 69×69×69 Å respectively. In each case, three combustion criteria namely with 250, 500, 1000 numbers of O₂ molecules having an equivalence ratio (φ) of 0.5, 1.008 and 2.0 respectively. This is also referred as fuel rich, stoichiometric and fuel lean combustion respectively. The system was minimized at a lower temperature of 10 K using NVE-MD ensemble simulation for all the coal molecules. The system was subsequently equilibrated with NVT ensemble at a temperature range of 2000-4000 K at an interval of 500 K for 200 ps. This is required since the combustion processes takes a longer time.³⁵ Using Berendsen thermostat, the temperature was controlled at a damping constant of 100 fs and 0.25 fs time step along with a total time of 200 ps. Similarly to analyze the intermediates and the products, a 0.3 bond order cut-off was used.

3. Results and Discussions

The simulation of the systems studied here should accurately model the coal systems with elastic bonds exhibiting translational, rotational, torsional, and vibrational motion. As a rule of thumb this requires a time step of an order of magnitude smaller than the shortest motion possible. This comes out to be approximately 0.1-0.25 fs. A smaller time step is

preferred with ReaxFF as the charges and bond orders are allowed to change at every time step. In reactive molecular dynamics, covalent bonds of reactant molecules involve breaking of old bonds and formation of new bonds. Bond breaking phenomena happens among only active functional groups. Those groups are predefined in the configuration script. The functional groups will be active only if it finds similar or dissimilar functional groups within a 'predefined' distance. For example, bond length of carbon-carbon single bond is ~1.54 Å. But in the configuration script, we decide the possible new bond formation when two such functional groups come within a distance much greater than this distance (say 6.0Å). But, our actual bond distance is much less than that. So to reduce the bond length from 6.0 Å to ~1.54Å⁴⁵ a huge amount of energy is generated. ReaxFF has a 'GUI' from which the user generates configuration script. ReaxFF here assumes a default value.

This necessitates a higher time or a lower time step to the system for the dissipation of this energy. In this case 1 fs time step will be quite large and newly formed bonds will have huge vibration. Thus the simulation will be unstable; hence a time step of 0.1 to 0.25 fs is usually used. This will slow down the events thereby negating higher energies. In the simulation of non-reactive systems (classical MD) we usually give a minimum time step of 1 fs unless we are dealing with proteins. In 1 fs time step, we do not use 'rigidBonds=all' command (refer to NPT/NVT configuration script written in NAMD) but we activate this option if the time step is more than 1 fs. This is performed to minimize the vibrations happening between C-H and other hydrogen containing bonds. Similar concept is also used in reactive molecular dynamics.^{25,27,28}

For high-temperature (~3000 K) simulations, a time step of 0.1 fs allows a proficient coverage of the phase space and collisions. This helps the reaction to come about smoothly. This has been usually the case for Ammonia-Borane decomposition which was studied

earlier.²⁴ In ReaxFF, we always maintain a balance between computational accuracy and computational time. The higher temperature is only given to the system to increase the velocity of molecules and thus to enhance the probability of faster collision. As mentioned previously, it is used to reduce the bond length to a user defined (or default value of program itself). This step creates a huge amount of energy which needs to be dissipated. To dissipate this energy, if the system as well as thermostat temperature is kept low, huge computational time will be required to control the set temperature. To optimize this time of computing, the simulation is run at an elevated temperature. This makes dissipation of heat consume lesser amount of time.²⁴⁻²⁵

A similar event was also observed by Wang et al.,³² where at high temperatures, the pathway of pyrolysis of *n*-dodecane to form H and *n*-C₁₂H₂₅ was observed. The dehydrogenation reaction of *n*-dodecane to form a H₂ molecule and an *n*-dodecane molecule was found to appear only once during their simulations, indicating that this reaction is hard to occur. Thus at lower temperature, it is difficult to determine the temperature effects on kinetics of different reactions. This would probably bring some uncertainty in mechanism analysis. Artificially increased temperatures were also employed in previous applications of ReaxFF MD^{32,37} and good agreement with experiment in the initial reaction products (such as CO and CO₂ which is our primary aim) were obtained. This is despite the time and temperature difference between ReaxFF MD simulations and experiments. With this we proceed with the discussion of section 3.1 and 3.2 involving the pyrolysis and the combustion process.

3.1 Combustion Analysis

3.1.1 Formation of CO and CO₂

Fig. 2 shows the general trend for the CO and CO₂ formation during the combustion analysis. In our previous work²³ with brown coal, we have obtained CO and CO₂ as the two major intermediates. The rate of reaction or formation is obtained by following equation;

$$R_{CO} = \frac{C_{CO}}{W} \times \dot{m} \tag{2a}$$

$$R_{CO_2} = \frac{C_{CO_2}}{W} \times \dot{m} \tag{2b}$$

Where C_{co} and C_{co_2} denotes CO and CO₂ concentration in mole of CO/kg of coal and mole of CO₂/kg of coal respectively. W is the weight of coal sample in kg and \dot{m} represents mass flow rates in kg of coal/ps respectively. The slope between concentration and time is usually written in chemical engineering terms as $\frac{dC_A}{dt}$. The rate of formation i.e $\frac{dC_{co}}{dt}$ and $\frac{dC_{co_2}}{dt}$ with CO and CO₂ concentration were obtained graphically. From the slope, it was found that both the reactions followed a first order mechanism (Eq. 3a and 3b). The negative sign implies that both gases are consumed in the reaction.

$$-\frac{dC_{CO}}{dt} = k[CO]$$
 (Eq. 3a)

$$-\frac{dC_{CO_2}}{dt} = k[CO_2]$$
 (Eq. 3b)

Here 'k' represents the rate constant in ps⁻¹ and takes the value 225.8 ps⁻¹ and 184.8 ps⁻¹ for CO and CO₂ respectively. This implies that the formation of CO is faster as compared to CO₂. This is further supplemented in Fig. 2 where it is observed that the rate of formation of

CO₂ is always higher than that of CO, which proves that CO₂ is the major intermediate gaseous product formed from the combustion of coal. This also agrees well with the previous experimental results.^{10-12,46,47}

The experimental and ReaxFF predicted rate of formation of CO and CO₂ is compared in Fig. 3(a) for CO and Fig. 3(b) for CO₂. While a qualitative match is found for CO, a quantitative agreement is found in CO₂. For chemical kinetic modelling, we usually adopt a closed homogeneous reactor with constraint volume and temperature in order to directly compare the results with ReaxFF. This has not been attempted in this work hence a qualitative trend was obtained in Fig. 3. A similar behaviour was also observed with the combustion of n-dodecane where the likely molecule in ReaxFF and kinetic modelling was ethylene, even though the quantitative results show larger deviations.³²

Thus the studies on coal using ReaxFF is beneficial in predicting the emission rate of gases for various rank of coal. In both the gases (CO and CO₂), the production rate reaches a maximum and then dies down gradually. Thus is due to the fact that initially the rate of formation of CO₂ and CO increases, thereafter it decreases as the oxygen concentration reaches it maximum value. Again it is observed that the rate of formation of CO₂ and CO is higher for lignite coal. This is primarily due to the large amount of oxygen present in the lignite version as compared to bituminous and anthracite coal. Further the magnitudes of formation rate of CO₂ and CO for lignite coal is higher than those of bituminous and anthracite coal. Fig. 4 shows the variation of CO/CO₂ ratio for lignite, bituminous and anthracite coal at different temperatures. It can be seen that for higher rank coal, the ratio of CO/CO₂ rapidly decreases with time which also agrees with experimental results ^{10,11} irrespective of temperature. Thus they are oxidized rapidly while reaching an asymptotic value. The variation in the production rate of CO to CO₂ ratio is also compared with experimental values in Fig. 5(a) for lignite and Fig. 5(b) for anthracite. It is evident that

production rate of CO₂ with respect to CO is enhanced with time and becomes constant which is a similar trend as per experimental studies. ^{10,11}

3.1.2 Computation of Activation Energies for CO and CO₂

To benchmark our modelling approach, an attempt has been made to calculate the activation energies for both CO and CO₂ for all the three varieties of coal. Table 1 shows the activation energy of CO and CO₂ formation for all the three coals which is obtained from the Arrhenius plots. An important observation is a close match in the activation energies for both CO and CO₂. It is also proven that the formation of CO is easier than CO₂ because of the lower activation energy. This also benchmarks our simulations against the reported data of Kaji *et al.*¹² and those obtained from the rate constants as given in equation 3(a) and 3(b). The smallest deviation in activation energies is observed for the bituminous coal. Table 2 discusses the formation of intermediates during the course of the reaction. Here it can be seen that the formation rate of CO is lower as compared to CO₂ molecules irrespective of temperature. However this should not be confused by the activation energies as the data presented below is at a time step of 175 ps.

It should be noted that the CO molecules are formed at the start of the reaction (lower activation energies) and tends to decrease with time. For lignite coal, a large quantity of CO and CO₂ molecules were released at a higher temperature. A similar phenomenon was also observed for anthracite and bituminous coal. In general, a large portion of CO and CO₂ molecules are formed at a temperature range of 3000-4000 K due to the higher interaction between the carbon atoms (either from coal or from CO) and oxygen molecules. It is proposed that CO molecules are formed by the breakage of aromatic rings and subsequent incomplete reaction with oxygen molecules. Thereafter the CO molecules directly react with O₂ to form CO₂ molecules which is depicted in Fig. 6. Intermediates such as H₂, H₂O, HCHO,

CH₃ and CH₄ are also formed during the course of the reaction. We now proceed in determining a reaction mechanism for the simplest of the coal molecule i.e. lignite.

3.1.3 Reaction Mechanism for Lignite Combustion

Fig. 6 shows the reaction mechanism of ReaxFF simulation at a temperature of 3000 K in fuel rich condition. It starts with an equilibrated structure of coal molecule (5 ps). As the coal molecules start to interact with oxygen molecules, it starts to divide into two aromatic like ring structure at a time step of 5.55 ps. The aromatic rings opens up to form straight carbon chain as 6.12 ps. Thus it is clear that the formation of CO is essentially due to the breakage of carbon-carbon (-C-C-) chain within the coal molecule. This also agrees with the lower activation energies as observed in a previous work¹² and our own comparison in Table 1. This is further supplemented in Fig. 7, where the production of CO starts earlier than CO₂ due to the breakage of -C-C- bond.

In the final stages, the carbon chain reacts with oxygen at a time step of 7.38 ps, where the first formation of CO is noticed. This is also accompanied by the release of the radical C_3HO_{\bullet} . The radical C_3HO_{\bullet} then reacts with O_2 molecule to form the remaining CO molecules at 8.36 ps. Simultaneously, this further releases the C_2H^{\bullet} (unstable) radical. In the concluding part the CO molecules tend to react with O_2 by forming the unstable form of carbon trioxide (CO_3) at 9.64 ps. This again reacts with O_2 and forms CO_2 at 13.44 ps with the abstraction of O_{\bullet} radical. Some of the valuable intermediate such as HCHO are formed after the reaction of CH_3 and CO_2 molecules at the end of simulation i.e. 57.28 ps. In the whole process the degradation of CO_2 molecules starts at 1.013ps (Fig. 7). This is mainly due to the effect of higher temperature thereby facilitating more collisions.

3.1.4 Effect of Temperature

Irrespective of the reaction mechanism, temperature and pressure only affects the reaction rates. In our previous work²³ we have reported that the temperature highly affects the oxidation process i.e. large numbers of gaseous intermediates are generated during the reaction. In a similar manner, Fig. 8 shows that as temperature increases, the formation rate of CO and CO₂ increases for all coal variant namely anthracite, bituminous and lignite. The formation rate of CO and CO₂ are found to be much higher at 4000 K as compared to lower temperature, which agrees with experimental observations. 10,11,48 It can be observed that the production rate of CO and CO₂ for anthracite is much higher than that of bituminous and lignite. This is due to the large number of carbon i.e. 45 carbons in anthracite coal as compared to 18 carbon present in bituminous coal and 39 carbons present in lignite coal. Therefore when the oxygen molecules react with high rank coal, oxygen and carbon present in the coal reacts to form large number of gaseous molecules such as CO and CO₂. The formation rate of CO and CO₂ initially increases but then decreases at a faster rate at higher temperature. This is due to the combustion process which proceeds at a faster rate at high temperature. ⁴⁹ The experimental variation for the rate of formation of CO and CO₂ for lignite coal is also compared in Fig. 9(a) for CO and Fig. 9(b) for CO₂. The ReaxFF predicted rates are smooth when compared to the experimental rates. However the trend and the order of magnitude do represent a similar trend i.e. the production of CO₂ picks up as the rate of formation declines for CO.

3.2 Product Formation in Pyrolysis Analysis

In the pyrolysis process, a large amount of gaseous products and intermediates are obtained. Gaseous product like CO_2 is a major component which is also obtained in the combustion process, as well as in our earlier work.²³ However valuable products like CH_4 , C_2H_4 and C_2H_6 are also evolved during the pyrolysis processes which agrees with the

experimental findings.¹² Table 3 gives us the amount of gaseous products such as CH₄, C₂H₄ and C₂H₆ evolved during the pyrolysis analysis at 3000 K for three different coals i.e. anthracite, bituminous and lignite. From Table 3, a larger amount of CH₄, C₂H₄, C₂H₆ are evolved in lignite and bituminous coals as compared to anthracite coal which agrees with the experimental trends.¹² Similarly, Table 4 shows the fraction of CO and CO₂ during the pyrolysis of anthracite, bituminous and lignite coal at 3500 K. The oxygen containing groups present in the coal decomposes to produce CO and CO₂. Fraction of CO₂ and CO were found to be 7.26 mole% and 14.52 mole% for lignite; and (6.45 mole% and 8.42 mole%) for bituminous coal respectively. This is higher as compared to anthracite coal on account of higher oxygen content present in low rank coals.¹² Hence as obvious during the decomposition, coal with higher oxygen content evolves more CO and CO₂.

Fig. 10 shows the amount of CO and CO₂ evolved during the pyrolysis at different temperature. The van't Hoff's plot i.e. Fig. 10 shows a linear plot of CO and CO₂ with respect to temperature. As per experimental trend, a linear relation for CO evolution is found for all the coal samples.¹² It implies that the oxygen containing group easily decomposes when pyrolised at 3500 K to produce CO₂. Table 4 gives the products of pyrolysis at 3500 K which depicts that the coal releases a higher content of CO and CO₂ and it depends on the rank of the coal.

Overall it is evident that the ReaxFF model (Figure 6) points out to the fact that the functional groups decompose to produce light gas species such as CO, CO₂, H₂, CH₂ and CH₄. Both the aromatic and aliphatic portion of coal releases the radicals H^{*} and OH^{*} in order to form CH₂, CH₄, CO and CO₂. The oxygenated coal molecules (CO, CO₂ and H₂O) and hydrocarbons (CH₃, CH₄, aliphatic) are hence the major intermediates formed during the reaction. In summary, the coal molecules fragment to produce unsaturated molecules and

hydrogen at a high temperature. This confirms the experimental reaction mechanism of Serio et al.,⁵⁰ for the pyrolysis reaction which includes gas phase reaction between non-hydrocarbon species. Further, it also depicts the gas phase reaction involving hydrocarbon species (paraffins and olefins) and hydrocarbon-non-hydrocarbon species (methane, CH₄). It also confirmed a gas-solid reaction involving char and non-hydrocarbon (CO, CO₂) which complements our ReaxFF MD-simulation results.

4. Conclusion

The combustion and pyrolysis of three different types of coals were analysed using ReaxFF molecular dynamics. The combustion analysis was done under fuel rich, stoichiometric and fuel lean conditions. Also, the pyrolysis was done under three different densities for lignite, bituminous and anthracite coals at a temperature range of 2000-4000 K. From the coal pyrolysis analysis, all the varieties of coal were found to produce light gas species such as CO, CO₂, H₂, CH₂ and CH₄. Oxygenated coal molecules (CO, CO₂ and H₂O) and hydrocarbons (CH₃, CH₄, aliphatic) were the major intermediates formed during the reaction. Thereafter the combustion and pyrolysis processes were compared with the experimental results and it was observed that ReaxFF results matches with the experimental findings in terms of rate of formation of CO and CO₂. This rate was higher for the lignite and bituminous coals as compared to anthracite coal. Also, in general the ratio of $\frac{CO}{CO_2}$ was found to decrease with time and has a higher ratio due to the rapid oxidation of oxygen containing groups. The activation energy for anthracite coal was found to be 59.2 kJ/mole for CO and 64.4 kJ/mole for CO₂ respectively. Similarly, the production rate of CH₄, C₂H₄ and C₂H₆ was also higher for lignite as compared to bituminous and anthracite coal.

Acknowledgement

The authors would like to thank the Council of Scientific and Industrial Research (CSIR), India for funding this project vide sanction letter no. 02(0093)/12/EMR-II. Useful discussions with Mr. Debashis Kundu, PhD scholar at Department of Chemical Engineering, IIT Guwahati is also acknowledged.

References

- 1. World Coal Association, Annual Energy Report, 2011, http://www.worldcoal.org/coal/.
- 2. D. W. van Krevelen, *Textbook of Coal: Typology, Physics, Chemistry, Constitution*, 3rd edn, Elsevier, 1990.
- 3. A. Kucuk, Y. Kadioglu and M. S. Gulaboglu, Combust. Flame, 2003, 133, 255-261.
- 4. Z. Li, Y. Wang, N. Song and Y. Yang, Procedia Earth Planet Sci., 2009, 1, 123-129.
- N. P. Vasilakos, *Textbook of Advances in Coal Chemistry*, Theophrastus Publications,
 S.A: Athens, Greece, 1988.
- 6. A. A. Agroskin, *Textbook of Chemistry and Technology of Coal*, Springfield, Va.: Jerusalem, 1966.
- H. Wang, B. Z. Dlugogorski and E. M. Kennedy, *Prog. Energy Combust. Sci.*, 2003, 29, 487-513.
- 8. N. M. Laurendeau, *Prog. Energy Combust. Sci.*, 1978, 4, 221-270.
- 9. G. S. Liu and S. Niksa, *Prog. Energy Combust. Sci.*, 2004, **30**, 679-717.
- 10. K. Baris, S. Kizgut and V. Didari, Fuel, 2012, 93, 423-432.
- 11. K. Baris, H. Aydin, and V. Didari, Combust. Sci. and Tech., 2011, 183, 105–121.
- 12. R. Kaji, Y. Hishinuma and Y. Nakamura, *Fuel*, 1985, **64**, 297-302.
- 13. S. R. Dhaneswar and S.V. Pisupati, Fuel Process. Technol., 2012, 102, 156-165.

- C. Moon, Y. Sung, S. Ahn, T. Kim, G. Choi and D. Kim, *Appl. Therm. Eng.*, 2013,
 111-119.
- 15. Y. Chen and S. Mori, *Energy Fuels*, 1995, **9**, 71-74.
- 16. S. Bhaskaran, A. Ganesh, S. Mahajani, P. Aghalayam, R.K. Sapru and D. K. Mathur, *Fuel*, 2013, **113**, 837-843.
- 17. I. Adanez-Rubio, A. Abad, P. Gayan, L.F. de Diego, F. Garcia-Labiano and J. Adanez, *Int. J. Greenh. Gas Con.*, 2013, **12**, 430-440.
- 18. K. Stanczyk, N. Howaniec, A. Smolinski, J. Swiadrowski, K. Kapusta, M. Wiatowski, J. Grabowski and J. Rogut, *Fuel*, 2011, **90**, 1953-1962.
- 19. T. Mendiara, F. Garcia-Labiano, P. Gayan, A. Abad, L.F. de Diego and J. Adanez, *Fuel*, 2013, **106**, 814-826.
- 20. C. K. Westbrook, W. J. Pitz, O. Herbinet, H. J. Curran and E. J. Silke, *Combust. Flame*, 2009, **156**, 181-199.
- 21. M. L. Hobbs, P. T. Radulovic and L. D. Smoot, *Prog. Energy Combust. Sci.*, 1993, 19, 505-586.
- 22. G. Domazetis, J. Liesegang and B. D. James, Fuel Process. Technol., 2005, 86, 463-486.
- 23. S. Bhoi, T. Banerjee and K. Mohanty, *Fuel*, 2014, **136**, 326-333.
- 24. M. R. Weismiller, A. C. T. van Duin, J. Lee and R. A. Yetter, *J. Phys. Chem. A*, 2010, **114**, 5485-5492.
- 25. A. C. T. van Duin, S. Dasgupta, F. Lorant and W. A. Goddard III, *J. Phys. Chem. A*, 2001, **105**, 9396-9409.
- 26. G. Domazetis, B. D. James and J. Liesegang, J. Mol. Model, 2008, 14, 581-597.
- 27. S. J. Stuart, A. B. Tutein and J. A. Harrison, J. Chem. Phys., 2000, 112, 6472-6486.

- 28. A. C. T. van Duin, A. Strachan, S. Stewman, Q. S. Zhang, X. Xu and W. A. Goddard, *J. Phys. Chem. A*, 2003, **107**, 3803-3811.
- 29. K. Chenoweth, A. C. T. van Duin and W. A. Goddard III, *J. Phys. Chem. A*, 2008, **112**, 1040-1053.
- 30. S. Agrawalla and A. C. T. van Duin, J. Phys. Chem. A, 2011, 115, 960-972.
- 31. E. Salmon, A. C. T. van Duin, F. Lorant, P. M. Marquaire and W. A. Goddard III, *Org. Geochem.*, 2009, **40**, 1195-1209.
- 32. Q. D. Wang, J. B. Wang, J. Q. Li, N. X. Tan and X. Y. Li, *Combust. Flame*, 2011, **158**, 217-226.
- 33. X. Liu, J. H. Zhan, D. Lai, X. Liu, Z. Zhang, and G. Xu, *Energy Fuels*, 2015, **29**, 2987-2997.
- 34. M. Zheng, X. Li, J. Liu and L. Guo, *Energy Fuels*, 2013, **27**, 2942-2951.
- 35. F. Castro-Marcano, A. M. Kamat, M. F. Russo Jr, A. C. T. van Duin and J. P. Mathews, *Combust. Flame*, 2012, **159**, 1272-1285.
- 36. F. Castro-Marcano and J. P. Mathews, *Energy Fuels*, 2011, **25**, 845-853.
- 37. F. Castro-Marcano, M. F. Russo Jr, A. C. T. van Duin and J. P. Mathews, *J. Anal. Appl. Pyrol.*, 2014, **109**, 79-89.
- 38. L. C. Liu, C. Bai, H. Sun and W. A. Goddard, *J. Phys. Chem. A*, 2011, **115**, 4941-4950.
- 39. B. Chen, X. Wei, Z. Yang, C. Liu, X. Fan, Y. Qing and Z. Zong, *Energy Fuels*, 2012, **26**, 984-989.
- 40. Scientific Computing & Modelling (SCM). ADF; SCM, Theoretical Chemistry, Vrije Universiteit: Amsterdam, Netherlands, 2013, http://www.scm.com.
- 41. J. P. Mathews and A. L. Chaffee, Fuel, 2012, 96, 1-14.

- 42. H. Kumagai, T. Chiba and K. Nakamura, *Prepr. Pap.–Am. Chem. Soc. Div. Fuel Chem.*, 1999, **44**, 633–637.
- 43. M. R. Narkiewicz and J. P. Mathews, *Energy Fuels*, 2008, 22, 3104–3111.
- 44. I. Wender, Catal. Rev.-Sci. Eng., 1976, 14 (1), 97–129.
- 45. B. Arab and A. Shokuhfar, J. Mol. Model., 2013, 19, 5053-5062.
- 46. M. Itay, C. Hill and D. Glasser, Fuel Process. Technol., 1988, 21, 81-97.
- 47. H. Wang, B. Z. Dlugogorski and E. M. Kennedy, *Energy Fuel*, 2003, **17**, 150-158.
- 48. D. L. Carpenter and G. D. Sergeant, *Fuel*, 1964, **43**, 247-266.
- 49. N. V. Marevich and A. B. Travin, *Otdl Tekh Nauk*, 1953, **1**, 1110-1117
- 50. M. A. Serio, D. G. Hamblen, J. R. Markham and P. R. Solomon, *Energy Fuel*, 1987, **1(2)**, 138–152.

FIGURE CAPTIONS

- **Fig. 1** Structure of (a) lignite coal $(C_{39}H_{35}O_{10}NS)$ (b) bituminous coal $(C_{18}H_{14}O)$ and (c) anthracite coal $(C_{45}H_{29}O_2NS)$ [Colour represents the different atoms such as yellow-Sulphur, blue-Nitrogen, gray-Carbon, red-Oxygen, white-Hydrogen atoms respectively (Mathews et al., 2012)⁴¹⁻⁴⁴].
- **Fig. 2** Variation in the formation rate of (a) CO₂ and (b) CO for three different coals at 3500 K from ReaxFF simulation results.
- **Fig. 3** Experimental and ReaxFF simulation results for formation rate of (a) CO and (b) CO₂ at 3500 K.
- **Fig. 4** Variation in CO/CO₂ ratio for (a) lignite (b) bituminous and (c) anthracite from ReaxFF simulation results.
- **Fig. 5** Variation in CO/CO₂ ratio for (a) lignite and (b) anthracite for experimental and ReaxFF results.
- Fig. 6 Reaction Mechanism of lignite at 3000 K from ReaxFF simulation.
- Fig. 7 Formation of CO and CO₂ molecules with time in ReaxFF simulation.
- **Fig. 8** The effect of temperature on the formation rate of CO, CO₂ for anthracite (a-b), CO, CO₂ for bituminous (c-d) and CO, CO₂ for lignite (e-f) from ReaxFF simulation results.
- **Fig. 9** Experimental and ReaxFF simulation results for the effect of temperature on the formation rate of (a) CO, (b) CO₂ for lignite.
- Fig. 10 Evolution of CO and CO₂ on pyrolysis of anthracite, bituminous, and lignite coal.

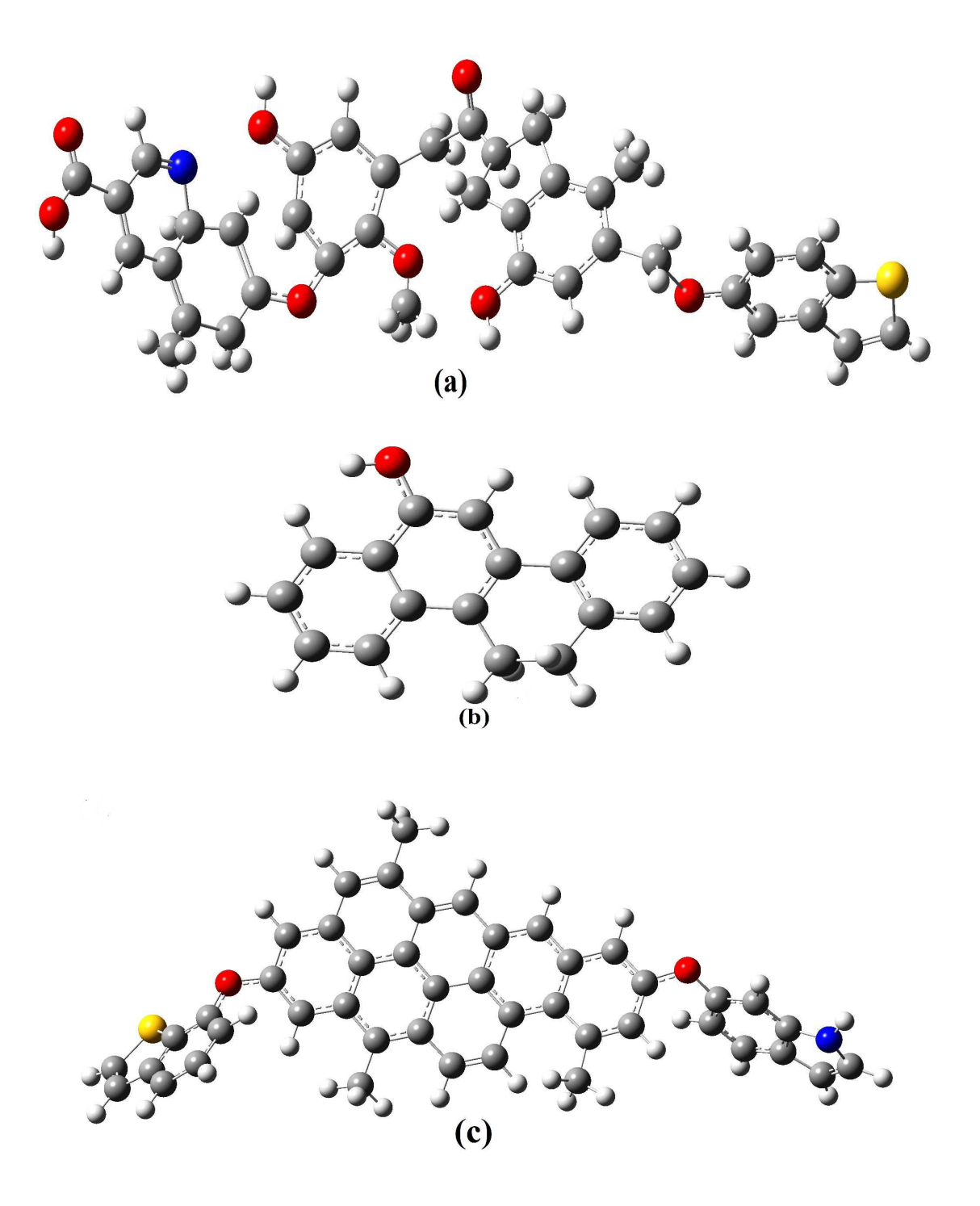
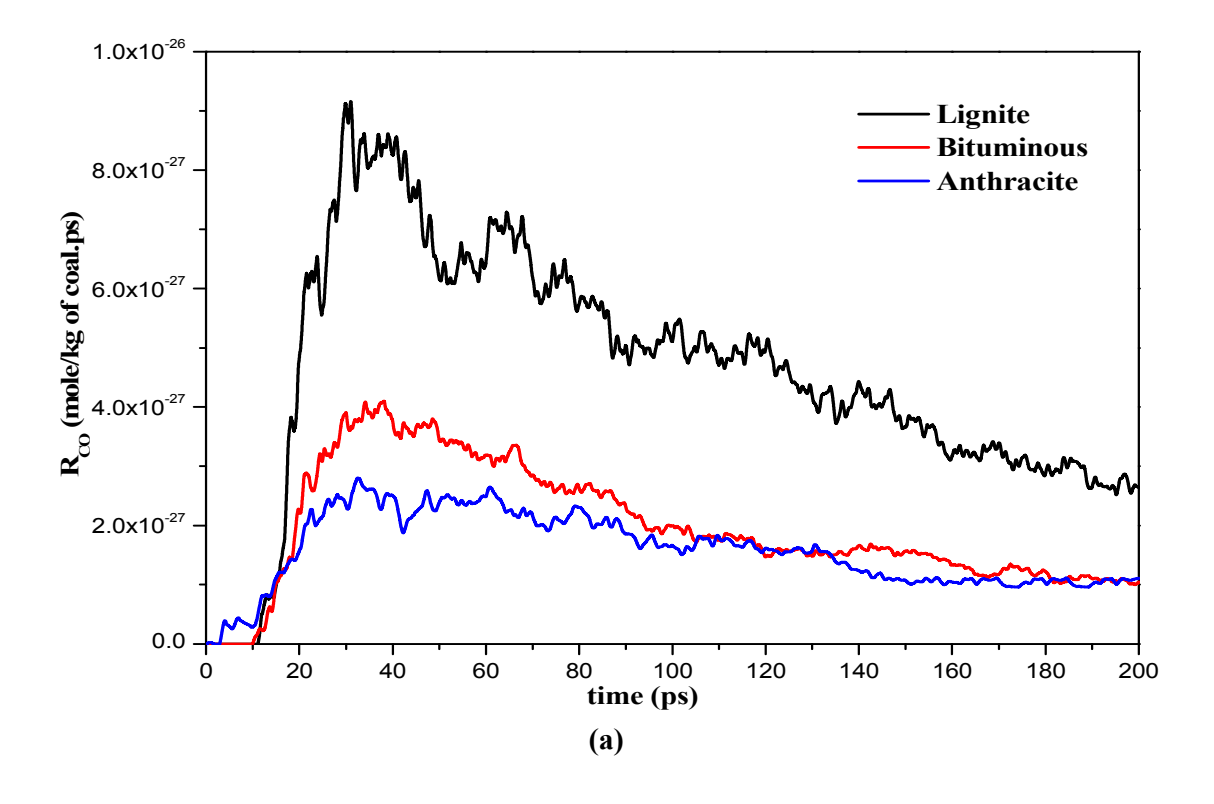


Fig. 1



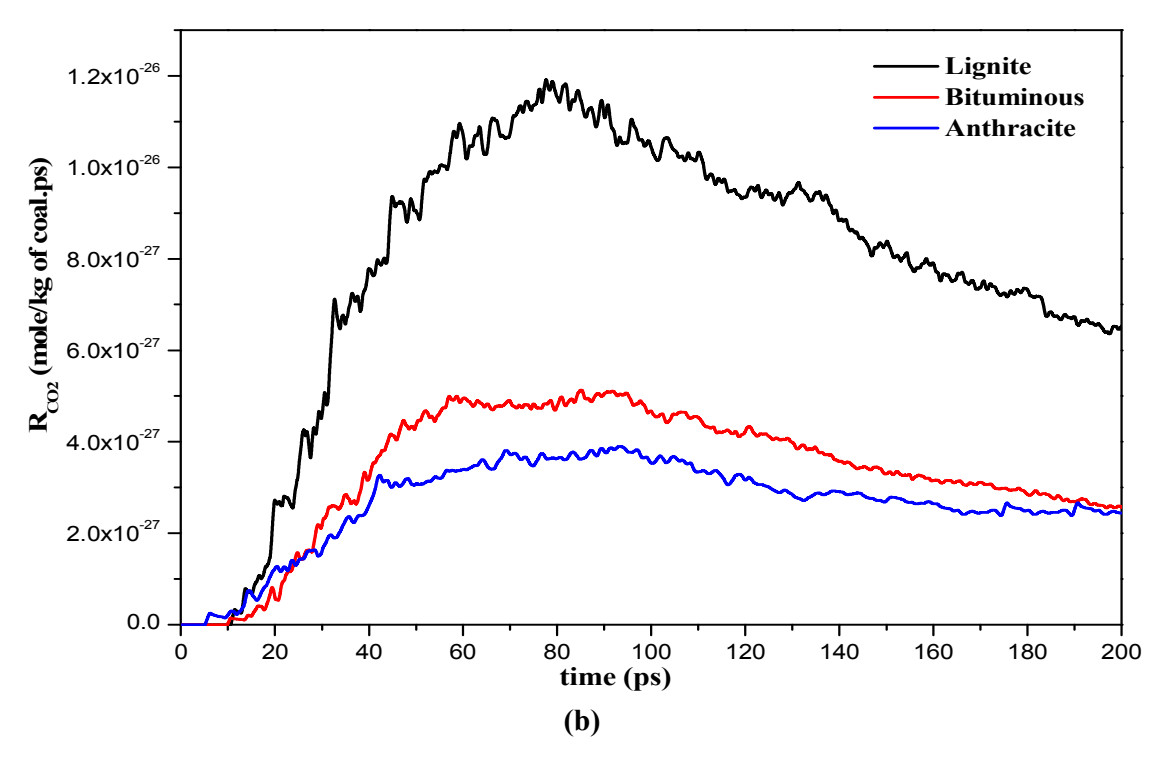


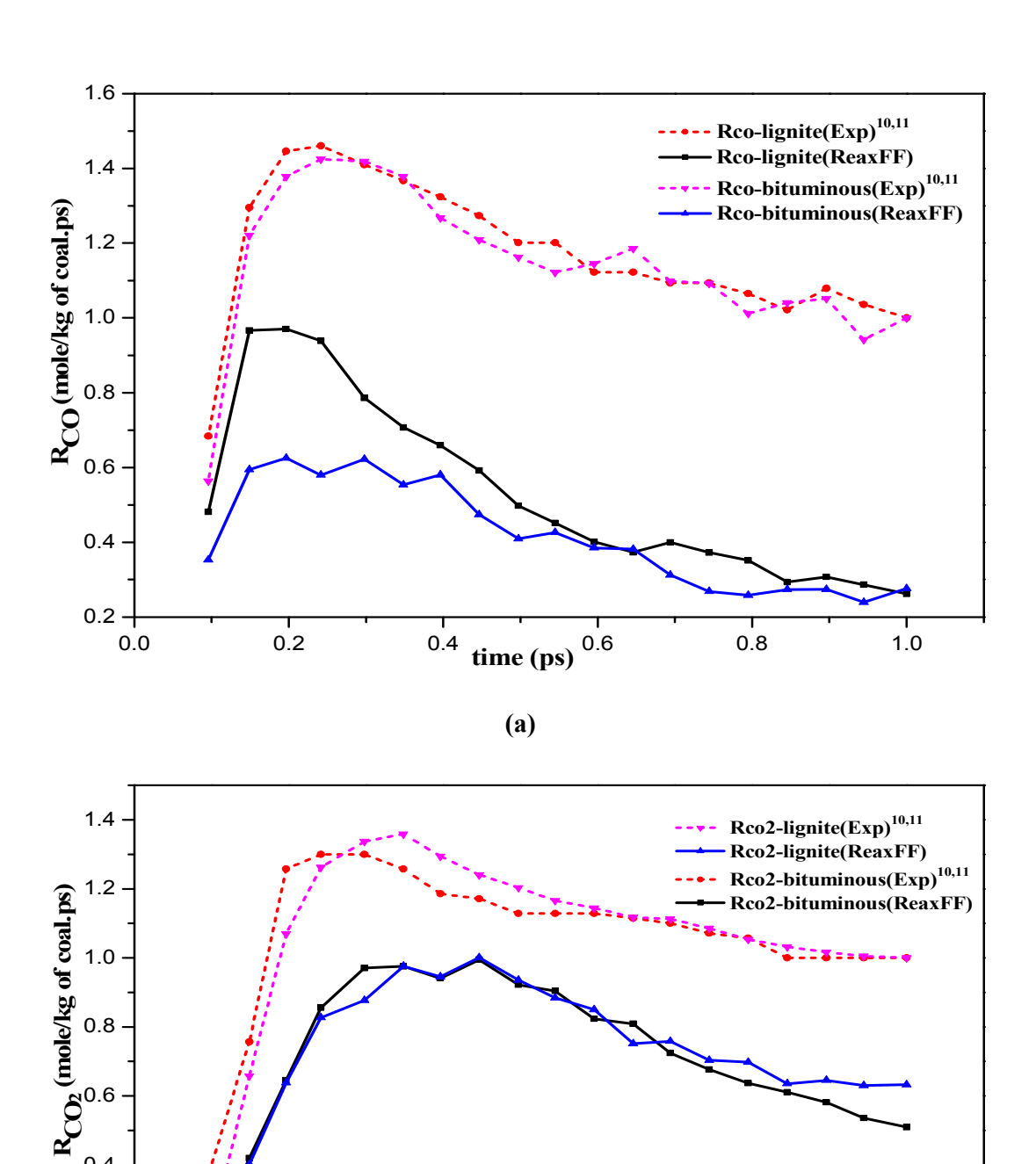
Fig. 2

0.4

0.2

0.0 +

0.2



(b)

Fig. 3

time (ps) 0.6

0.8

1.0

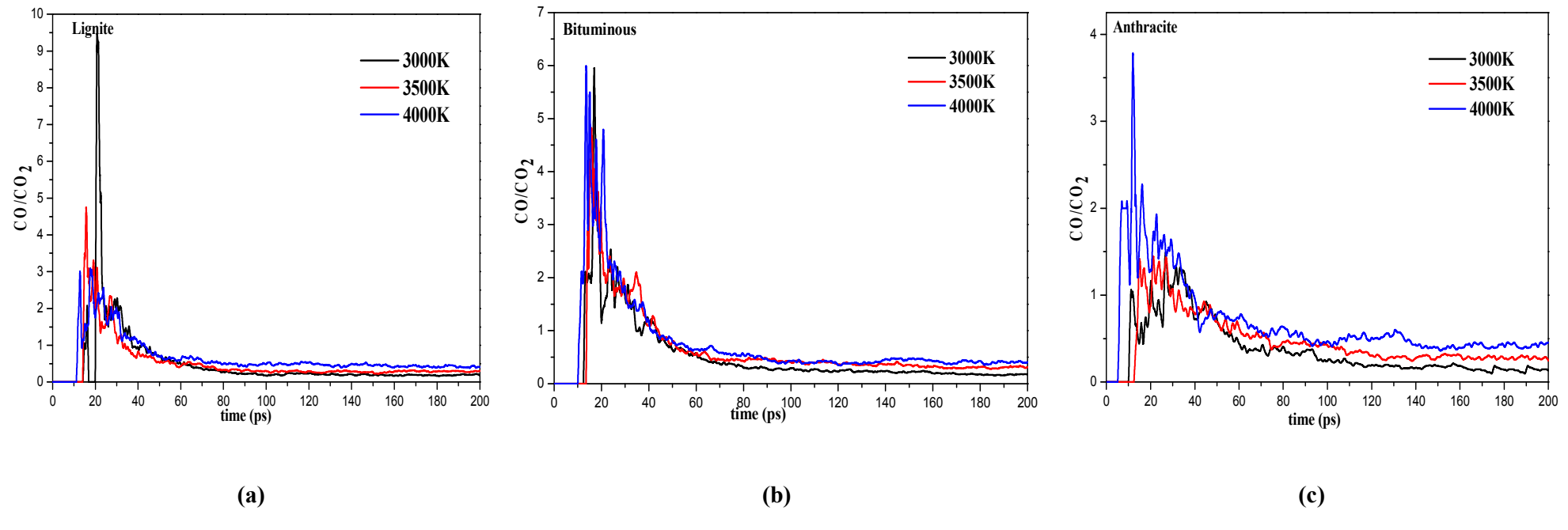


Fig. 4

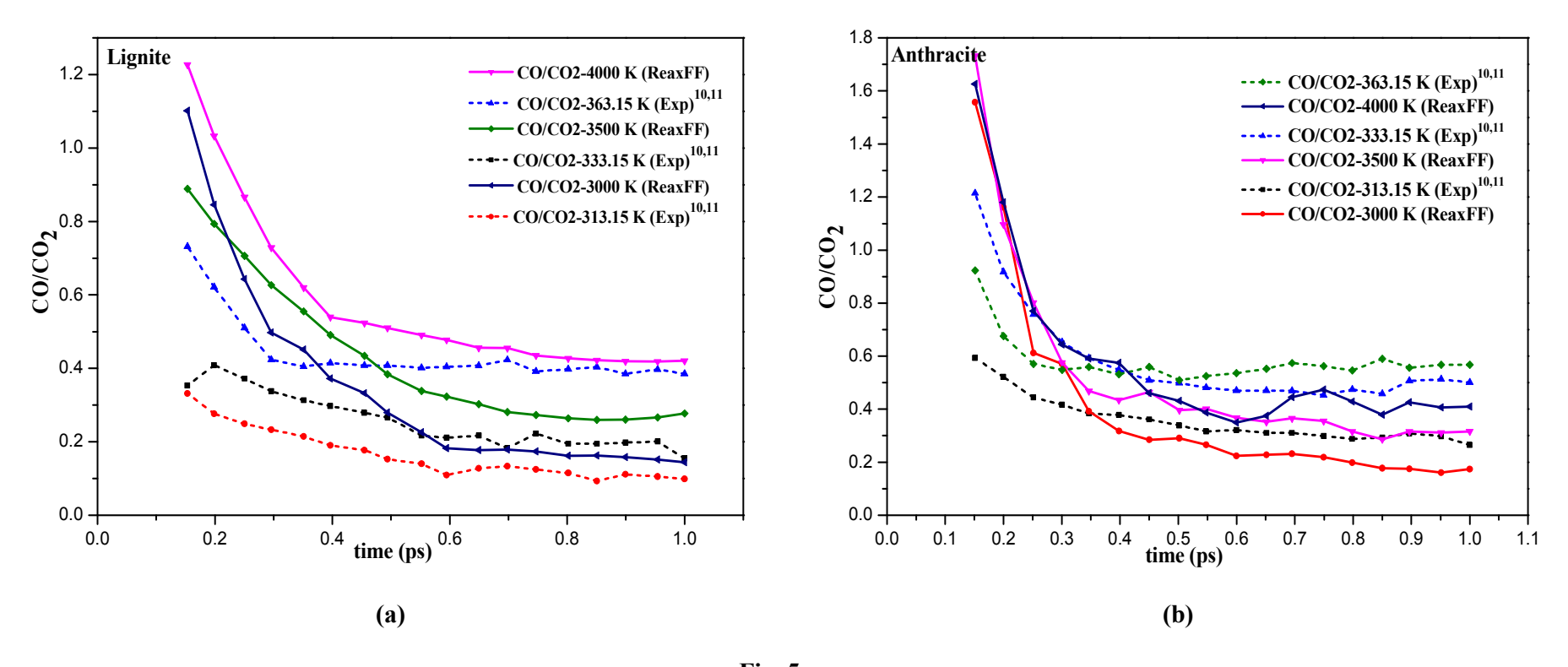


Fig. 5

Fig. 6

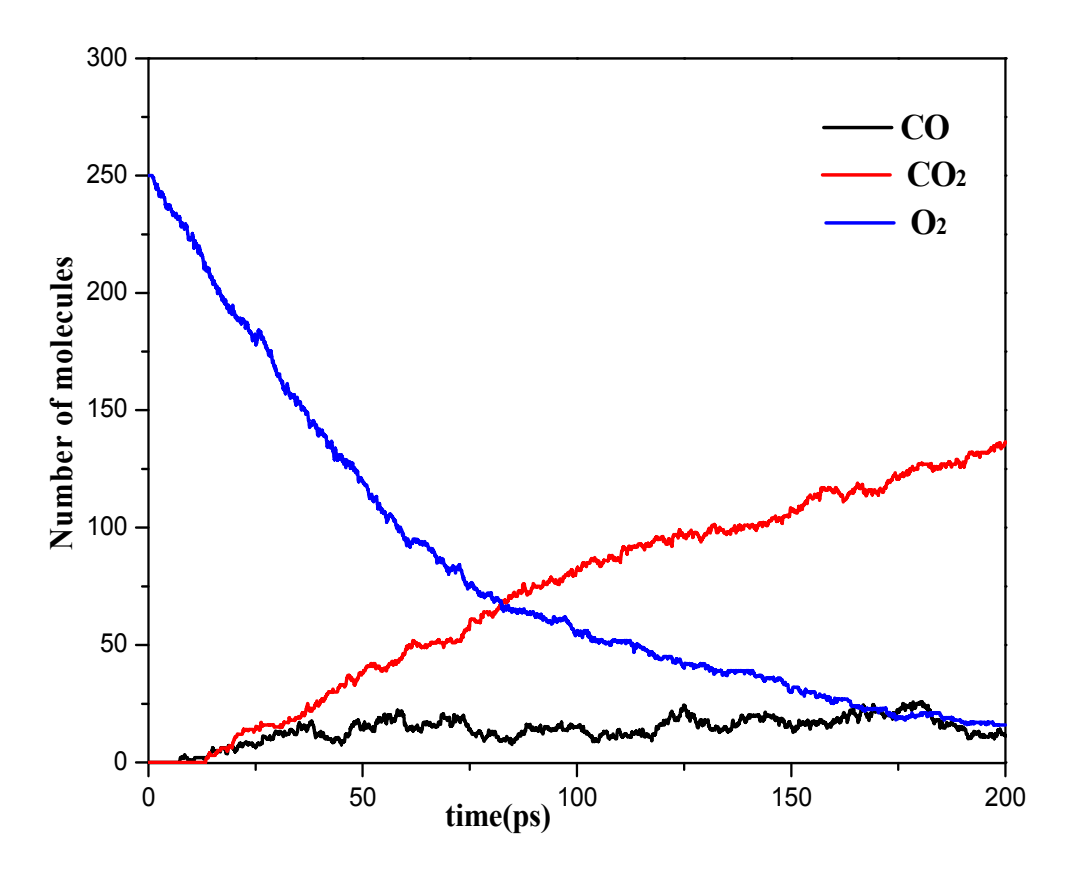
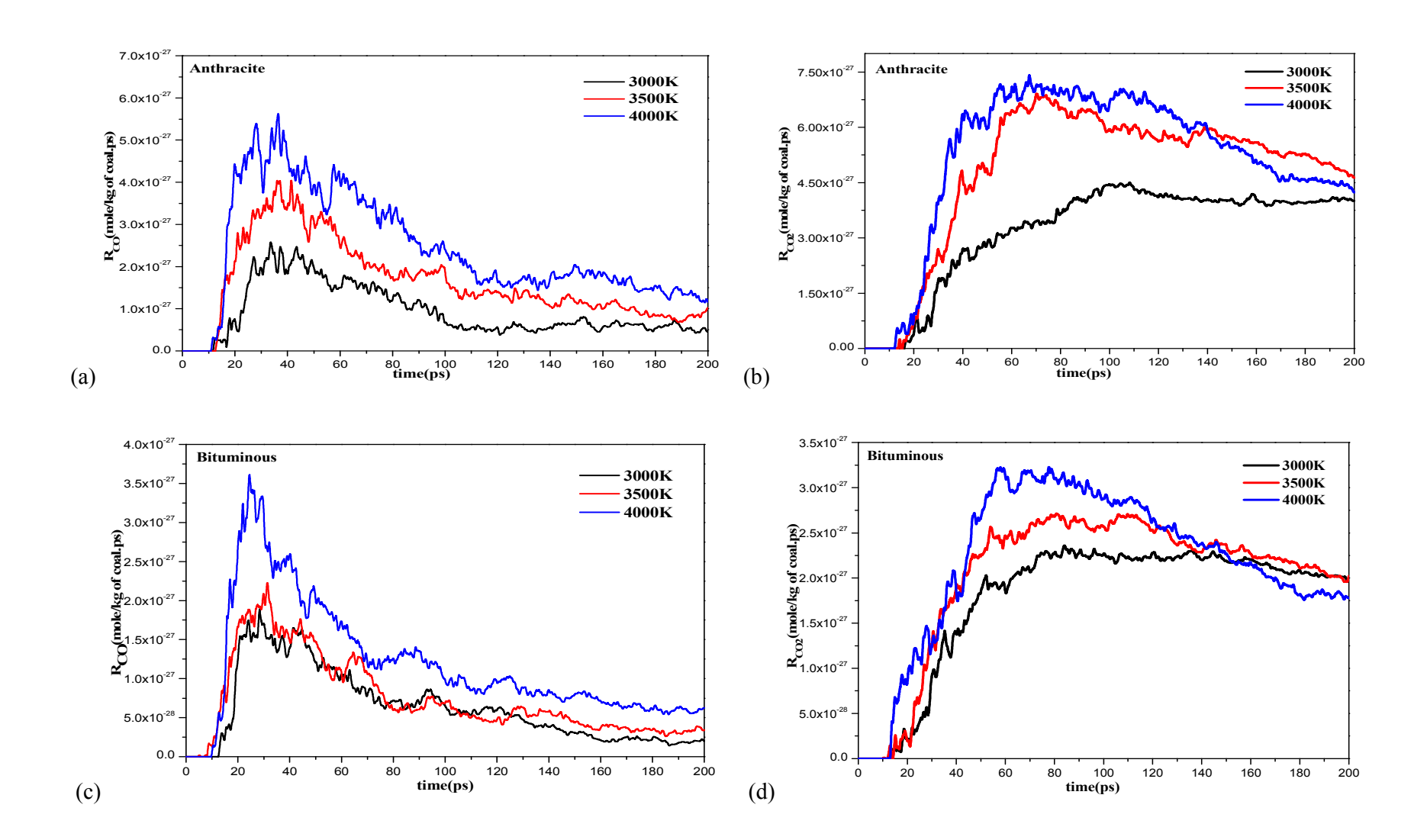


Fig. 7



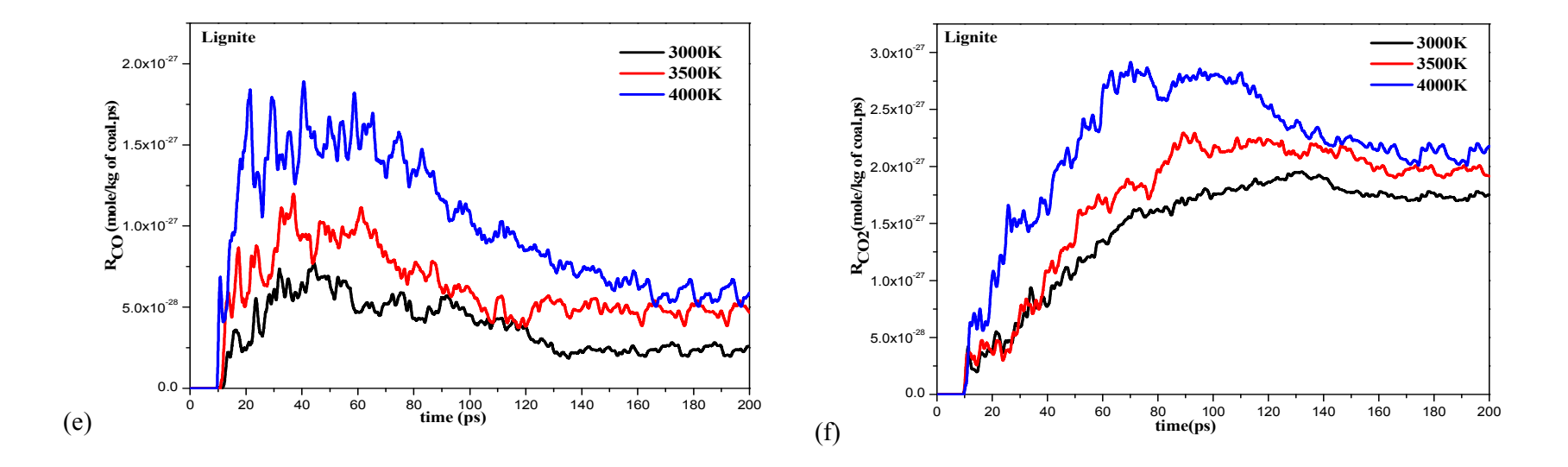


Fig. 8

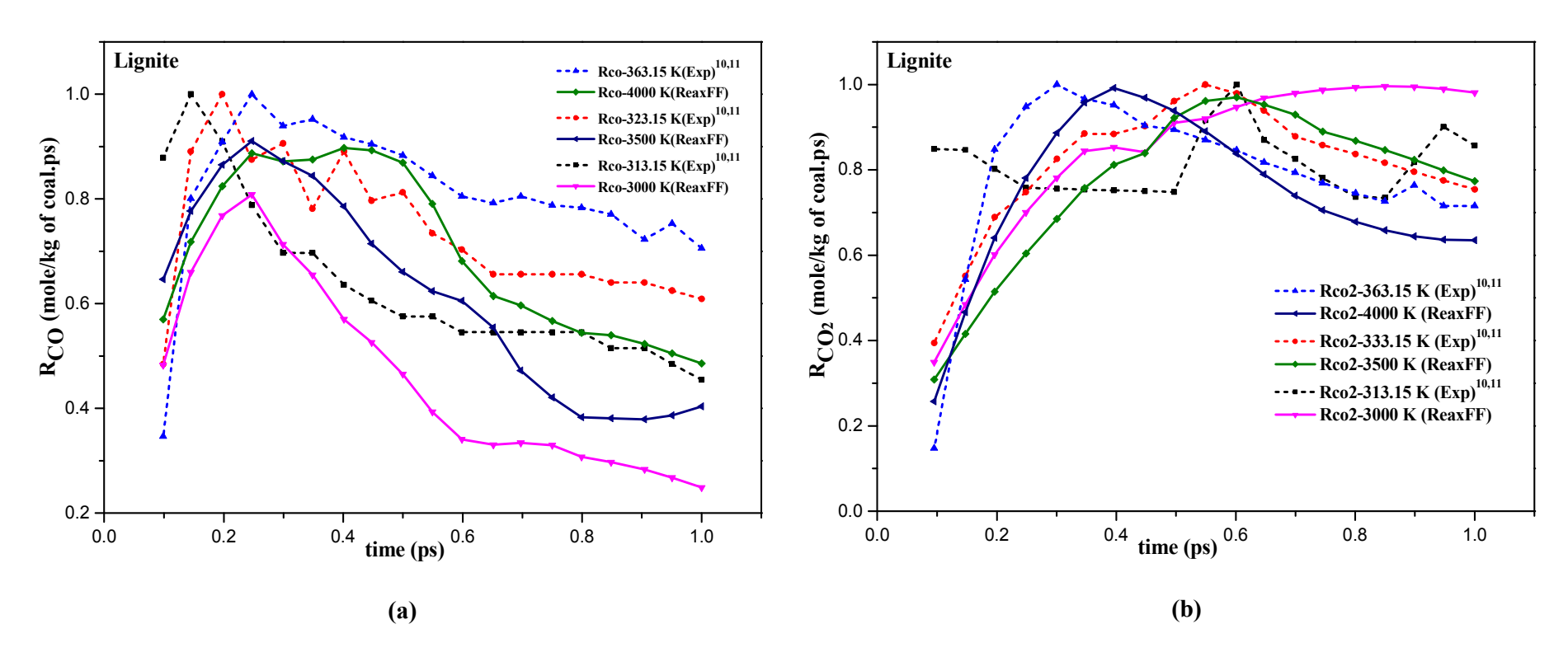
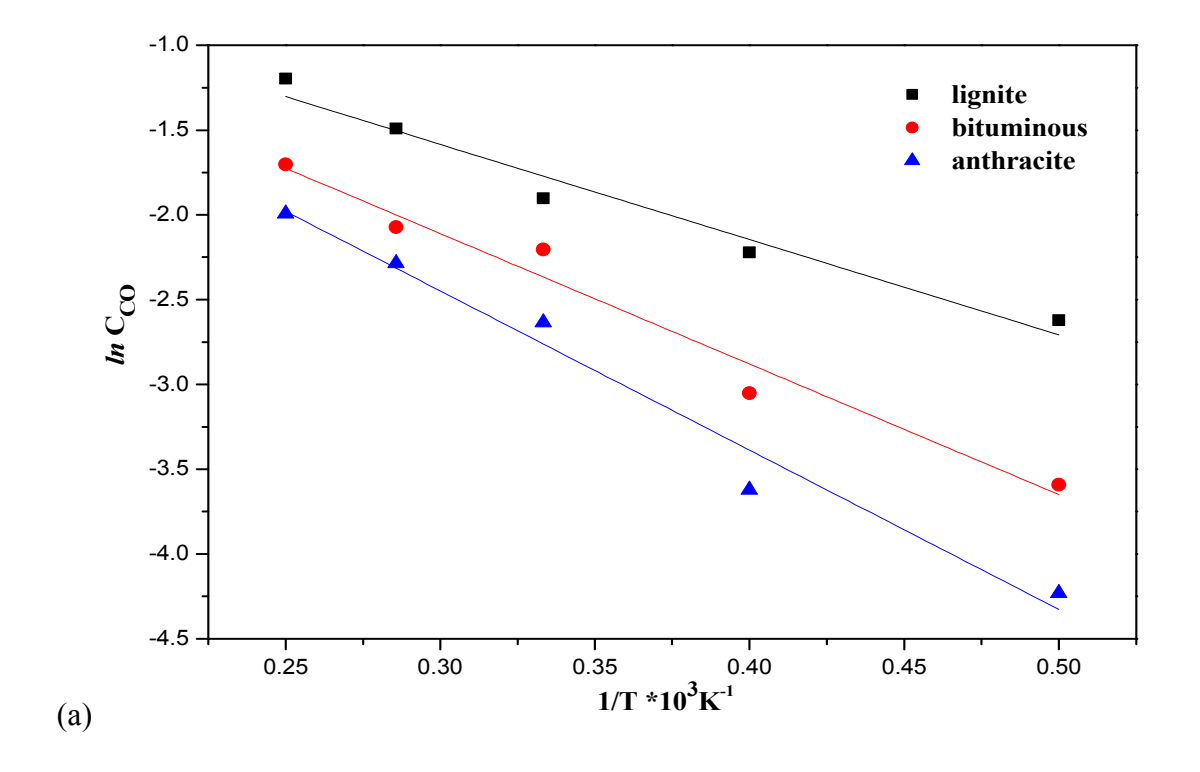


Fig. 9



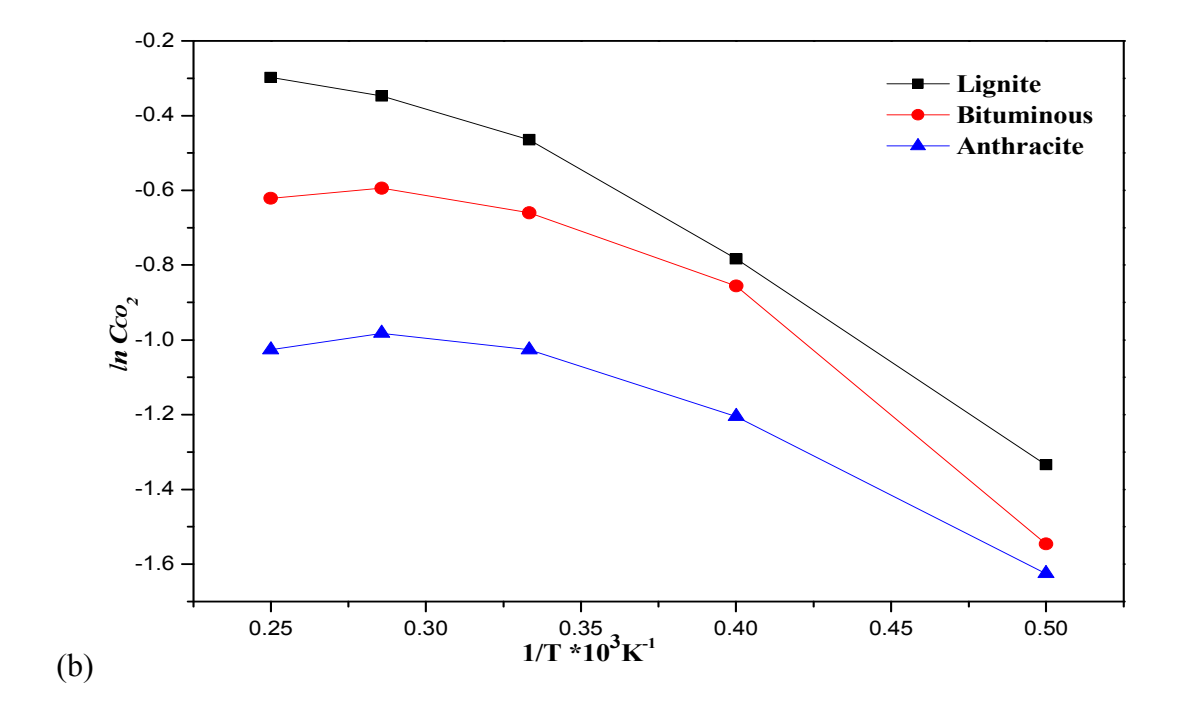


Fig. 10

Table 1. Activation energy (E) of CO and CO₂ at 150 ps for combustion process

Types of coal	E _{CO} (kJ/mole) (ReaxFF)	E _{CO} (kJ/mole) (Experimental ¹²)	Ea _{CO2} (kJ/mole) (ReaxFF)	E _{CO2} (kJ/mole) (Experimental ¹²)
Lignite	46.1	51.5	56.4	56.1
Bituminous	52.1	54.4	60.5	59.4
Anthracite	59.2	58.2	64.4	59.4

Table 2. Formation of valuable intermediates at 175 ps for lignite formed during ReaxFF simulation

Temperature (K)	CO	CO_2	H ₂	H ₂ O	НСНО	CH ₃	CH ₄
2000	18	154	2	42	17	2	0
2500	29	272	2	63	18	0	1
3000	93	321	2	57	10	0	0
3500	93	321	2	57	6	1	1
4000	113	284	6	43	2	2	3

Table 3. Industrially relevant gas as evolved in pyrolysis at 3000 K

Types of coal	CH ₄ (mole %)	C ₂ H ₄ (mole %)	C ₂ H ₆ (mole %)
Lignite	8.0645	22.5806	8.0645
Bituminous	6.4516	18.3140	6.4516
Anthracite	5.6451	11.2903	3.7058

Table 4. Fraction of coal- O_2 evolved as CO_2 and CO on pyrolysis at 3500 K

Types of coal	CO ₂ (mole %)	CO (mole %)
Lignite	7.2580	14.5161
Bituminous	6.4516	8.4193
Anthracite	5.6451	1.6129